DOI:10.1190/image2022-3751334.1

Efficient acquisition and imaging of high-resolution seismic data with the continuous wavefields method

Tilman Klüver (PGS) and Torben Høy (PGS)*

Summary

The continuous wavefields method allows the simultaneous operation of multiple sources in a seismic experiment and efficient separation of the wavefields emitted by different sources. This method provides significant improvements in source-side sampling both inline and crossline without penalty on acquisition efficiency. We demonstrate a processing flow that is designed to preserve high temporal and spatial bandwidth for high-resolution seismic imaging of data acquired with the continuous wavefields method. We illustrate it with data examples acquired offshore Brazil.

Introduction

The continuous wavefields method utilizes continuous emission of energy on the source side and continuous recording of the wavefield on the receiver side (Hegna et al., 2018a). The method significantly reduces the emitted sound pressure and exposure levels compared to conventional acquisition techniques and allows for effective simultaneous operation of multiple sources (Hegna et al., 2018b). Previous publications have introduced the methodology and principles behind it and illustrated these with field data examples; however, all data examples have hitherto been limited to 4 ms temporal sampling rate and the associated temporal and spatial bandwidth.

In this paper, we present results that extend the temporal and spatial bandwidth beyond the limits previously shown to generate images relevant to, for example, shallow hazard analysis or carbon capture and storage monitoring. We use a data set acquired offshore Brazil to demonstrate how the use of continuous wavefields during acquisition supports processing and imaging of the data to provide a high-resolution image with 2 ms temporal sampling. Starting with acquisition aspects, we will describe the processing route taken to obtain high resolution images.

The continuous wavefields method

The method utilizes continuous wavefields on both the source and the receiver side. All data recorded over the length of a sail-line constitutes the continuous wavefield on the receiver side and is processed as one long record. On the source side, individual air-guns are triggered with dense randomized time intervals such that one air-gun is triggered every 200-300 ms on average. In this way, energy is emitted near-continuously allowing for dense inline sampling along source trajectories. Since only a single air-gun is triggered at any point in time, the emitted wavefield has point source characteristics. The absence of directivity and related notches in the wavenumber spectrum, as introduced with traditional air-gun arrays, contributes to high lateral resolution. The emitted source wavefield approaches the properties of band-limited white noise, thereby generating a very strong encoding which allows simultaneous operation of many sources and the separation of their emitted wavefields during processing. Simultaneous operation of multiple sources in different crossline positions is necessary for efficient acquisition of data with dense crossline CMP spacing. The continuous emission of energy from all sources means that, in contrast to traditional blended acquisition, there is no listening time requirement to obtain a clean record. Consequently, there is no speed limit imposed on acquisition by the method as such.

Data acquisition

The data set used in this paper was acquired in 2018 offshore Brazil in a deep-water setting (Klüver et al., 2019). The map shown in Figure 1 indicates the survey location. The survey consists of eight sail-lines with an approximate length of 25 km. The data were acquired using 16 multisensor streamers with 8 km length that were spaced 100 m apart and towed at 15 m depth. Six source arrays were deployed spaced 16.67 m apart in the crossline direction and located in a central crossline position in front of the streamer spread at 6 m depth. This layout results in a total of 96 CMP lines distributed over 800 m crossline coverage per sail-line. Nominal crossline CMP bin size in acquisition is 8.33 m. The acquisition layout is illustrated in Figure 2.

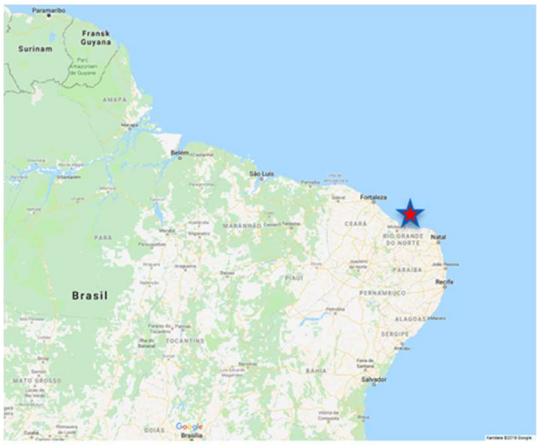

Figure 1: Survey location in the northern part of Brazil offshore Fortaleza.

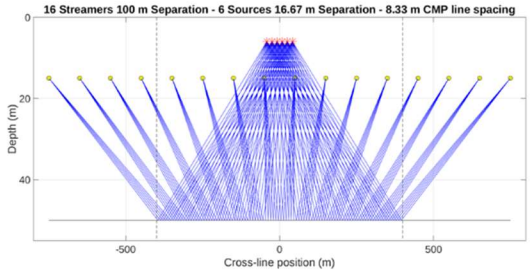

Figure 2: Source and streamer configurations.

Each of the six source arrays consists of a single string equipped with six air-guns. The source layout is shown in Figure 3. There are air-guns with three different volumes on each string. The volumes have complementary bubble periods such that the emitted source wavefield can be deconvolved in a robust fashion from the data without deep bubble related notches in the deconvolution operator that would cause instability. The six air-guns are arranged differently on each string to minimize correlation between wavefields emitted by different strings. The air-guns are triggered in a pre-defined sequence with dense randomized time intervals giving a mean trigger time interval of 290 ms between successive triggerings. A near-field recording system continuously records the emitted wavefield.

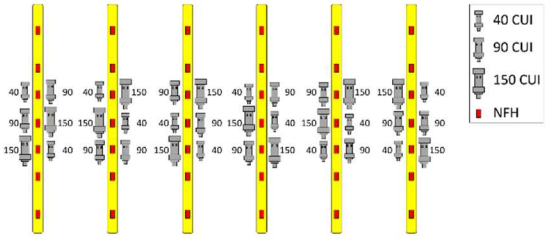

Figure 3: Hexa-source layout with a different arrangement of complementary air-gun volumes on each string.

Since energy is emitted near-continuously from all sources, the shot point interval along the sail-line becomes a processing parameter that can be chosen to optimally support broadband processing for high-resolution imaging. There is no need for a pre-defined shot point interval determined by trading off number of sources operated, clean record length, fold, and vessel speed.

Figure 4 shows a five-second-long segment of hydrophone data recorded continuously on one of the sail-lines. The density of air-gun triggerings can readily be seen in the figure.

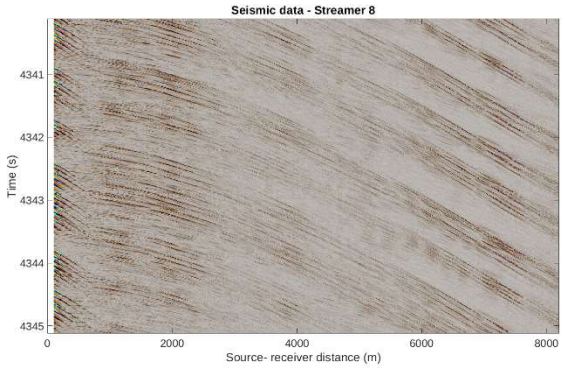

Figure 4: Five seconds long segment of a continuous hydrophone record.

Data processing

The processing sequence follows the lines described in Klüver et al. (2018). There is a step added for spatial up-sampling on the receiver side which mitigates spatial aliasing due to 12.5 m channel spacing.

The continuously recorded near-field hydrophone data is used to determine a unique notional source signature for every air-gun triggering that occurred in the field. With only a single air-gun being triggered at any point in time and its emitted wavefield being recorded by multiple near-field hydrophones on each string, it is possible to accurately account for small variations in the notional signatures due to, for example, small pressure fluctuations in the air supply and changes in the surroundings of the source.

The streamer data is recorded continuously in the field. The first processing step is to deconvolve all acquisition system related filter responses from the data including the sensor responses of pressure and particle motion sensors. The particle motion data is converted to its pressure equivalent by multiplying with acoustic impedance.

In the next step, the previously determined notional source signatures are used to predict the recorded direct arrival events and attenuate them from both pressure and particle motion recordings.

Noise attenuation is then applied to the continuous data using a method that exploits the long continuous records.

The next step in the processing sequence is the receiver motion correction. The data is first up-sampled on the receiver-side from the 12.5 m channel spacing recorded in the field to 6.25 m to mitigate incorrect handling of spatially aliased energy. The receiver motion correction applies a spatial phase shift to the continuous data to correct for motion of the towed equipment along the sail-line. This

transforms the data as if it had been recorded in stationary positions in the field. The output of this step is a set of stationary receiver traces spaced 6.25 m along the sail-line trajectory. Due to deviations from nominal geometry such as streamer feathering, the data does not end up in truly stationary receiver positions; however motion along the line is minimized and deviations from truly stationary positions are smooth, gradual and small over typical conventional record lengths of a few of tens of seconds.

The receiver motion correction is followed by the receiver-side wavefield separation into up-going and down-going pressure by combining pressure and particle motion recordings. The receiver-side wavefield separation is performed on the long continuous records.

The last method-specific processing step is the multi-dimensional deconvolution of the source wavefield from the receiver traces. This is done in an iterative fashion accounting for accurate positioning of the sources relative to the data in the receiver traces. We choose an output source point spacing of 6.25 m for every source to obtain symmetric sampling of source and receiver positions in the inline direction. The output of the source deconvolution is a set of receiver gathers, one for each source, spaced 6.25 m along the sail-line and with 6.25 m trace spacing within each gather.

This data can be sorted to a traditional shot gather geometry with 6.25 m shot point interval along every individual source line and with 6.25 m channel spacing. This results in significantly improved inline shot point sampling: a traditionally blended hexa-source acquisition with one shot every 6.25 m would have 37.5 m shot point interval per source line.

From this point onwards, standard processing techniques are applied.

Results

The output data from the source deconvolution were normal moveout corrected and stacked on a grid with bin sizes of 3.125 m in the inline and 8.33 m in the crossline direction. While the inline direction is free of signs of spatial aliasing, there remain aliased events in the crossline direction as illustrated in the f-k spectrum shown in Figure 5. This example demonstrates that the nominal crossline CMP spacing of 8.33 m, despite being significantly finer than obtained using traditional acquisition geometries, is still insufficient to image very shallow events without spatial aliasing.

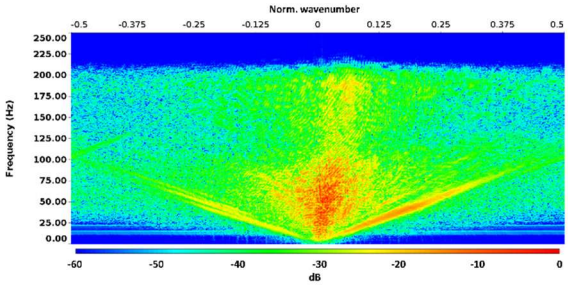

Figure 5: F-k spectrum of a crossline section after 3D NMO and stack. There clearly remains spatially aliased energy in the crossline direction with the nominal bin size provided by the acquisition layout.

The stacked data was 3D post-stack time migrated followed by application of source-side deghosting. Figure 6 shows a 5 km long part of an inline section, illustrating the shallow structural complexity in the data. It is also evident that the large shallow bandwidth quickly decreases with depth due to attenuation.

As illustrated in Figure 5, there remains spatially aliased energy in the crossline direction. To illustrate the achievable bandwidth and hence the potential in the data, we show the result of regularization for offsets between 1000 m and 1100 m. All traces within that 100 m offset range have been regularized and up-sampled in the crossline direction to generate a single-fold cube with 3.125 m inline and 4.166 m crossline trace spacing. Figure 7 shows a crossline and an inline section of the single fold data set. Figure 8 shows the f-k spectra associated with the red windows highlighted in Figure 7. These f-k spectra demonstrate that spatial bandwidth recovered from the data can be extended beyond the Nyquist wavenumbers for the natural 6.25 m inline trace spacing and 8.33 m crossline trace spacing.

Conclusions

We have extended the processing flow for data acquired with the continuous wavefields method such that it provides the large temporal and spatial bandwidth needed to generate high-resolution seismic images. The data used to illustrate our results have been acquired very efficiently with a streamer layout typically deployed for exploration-type surveys. The continuous wavefields method allows the operation of multiple sources simultaneously thereby improving the source-side sampling in both the inline and crossline direction. This is a key enabler for achieving the results shown. The improved inline source side sampling comes without any penalty on acquisition speed as encountered in traditional blended acquisition techniques where inline shot point interval and number of sources typically are traded against clean record length and desired fold.

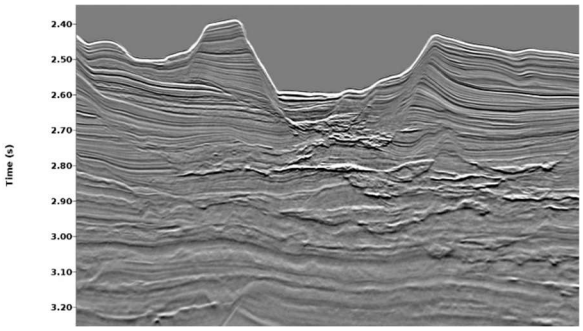

Figure 6: Time migrated inline section illustrating structural complexity.

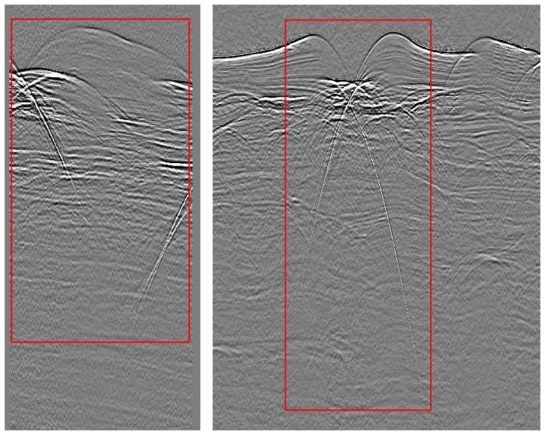

Figure 7: Crossline (left) and inline (right) section from the single-fold cube after regularizing all traces with offsets between 1000 m and 1100 m. The temporal extent of the sections is about 1.2 s.

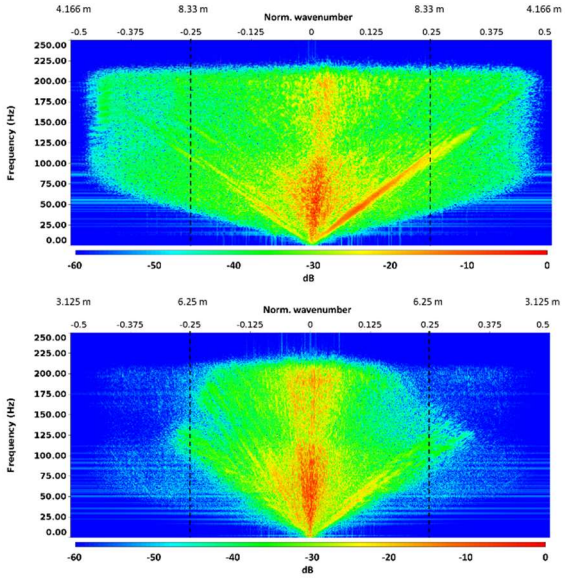

Figure 8: F-k spectra for the windows highlighted in Figure 7. Top: crossline section. Bottom: inline section. The trace spacing for different wavenumbers is annotated above the normalized wavenumber axis.

Acknowledgements

The authors like to thank PGS for permission to publish this work. Special thanks go to the crew of Ramform Tethys for acquiring the data in an efficient and safe manner. We are grateful for fruitful discussions with and support from PGS Imaging department.

REFERENCES

Hegna, S., T. Klüver, and J. Lima, 2018a, Making the transition from discrete shot records to continuous wavefields — Methodology: 80th Annual International Conference and Exhibition, EAGE, Extended Abstracts, We A10 03, doi: https://doi.org/10.3997/2214-4609.201800998.

Hegna, S., T. Klüver, and J. Lima, 2018b, Benefits of continuous source and receiver side wavefields: 88th Annual International Meeting, SEG, Expanded Abstracts, 41–45, doi: https://doi.org/10.1190/segam2018-2995322.1.

Klüver, T., S. Hegna, and J. Lima, 2018, Processing of data with continuous source and receiver side wavefields — Real data examples: 88th Annual International Meeting, SEG, Expanded Abstracts, 4045–4049, doi: https://doi.org/10.1190/segam2018-2995339.1.

Klüver, T., S. Hegna, and J. Lima, 2019, Results from a 3D field trial with a seismic acquisition and processing method based on continuous wavefields: 89th Annual International Meeting, SEG, Expanded Abstracts, 4751–4755, doi: https://doi.org/10.1190/segam2019-3215502.1.